frontiers | Frontiers in Physics

ORIGINAL RESEARCH
published: 06 July 2022
doi: 10.3389/fphy.2022.934848

Design of a High-Speed OFDM-SAC-OCDMA-Based FSO System Using EDW Codes for Supporting 5G Data Services and Smart City Applications

Mehtab Singh[1], Jan Kříž[2], M. M. Kamruzzaman[3], Vigneswaran Dhasarathan[2], Abhishek Sharma[4] and Somia A. Abd El-Mottaleb[5]*

[1]Department of Electronics and Communication Engineering, University Institute of Engineering, Chandigarh University, Mohali, India, [2]Department of Physics, Faculty of Science, University of Hradec Králové, Hradec Králové, Czechia, [3]Department of Computer Science, College of Computer and Information Sciences, Jouf University, Sakakah, Saudi Arabia, [4]Department of Electronics Technology, Guru Nanak Dev University, Amritsar, India, [5]Alexandria Higher Institute of Engineering and Technology, Alexandria, Egypt

OPEN ACCESS

Edited by:
Muhammad Saadi,
University of Central Punjab, Pakistan

Reviewed by:
Shanmuga Sundar Dhanabalan,
RMIT University, Australia
Ayyanar Natesan,
Thiagarajar College of Engineering, Madurai,India

***Correspondence:**
Mehtab Singh
mehtab91singh@gmail.com

Specialty section:
This article was submitted to Optics and Photonics, a section of the journal Frontiers in Physics

Received: *03 May 2022*
Accepted: *27 May 2022*
Published: *06 July 2022*

Citation:
Singh M, Kříž J, Kamruzzaman MM, Dhasarathan V, Sharma A and Abd El-Mottaleb SA (2022) Design of a High-Speed OFDM-SAC-OCDMA-Based FSO System Using EDW Codes for Supporting 5G Data Services and Smart City Applications. Front. Phys. 10:934848. doi: 10.3389/fphy.2022.934848

A novel free space optics (FSO) system is introduced in this article by combining orthogonal frequency division multiplexing (OFDM) with spectral amplitude coding optical code division multiple access (SAC-OCDMA) to be implemented in 5G technology and smart cities. Enhanced double-weight (EDW) codes are used as signature codes, while for the detection technique, single photodiode detection (SPD) is applied for the SAC-OCDMA system. OFDM with a four-quadrature amplitude modulation (4-QAM) scheme is assigned to the three users in the SAC-OCDMA system, each carrying 15 Gbps. Adverse weather conditions, such as clear, fog, haze, rain, and dust storm, that affect the FSO channel are considered. The performance of the proposed system is evaluated in terms of log of bit error rate and received power at different propagation distances. The simulation results show successful transmission of 3 × 15 Gbps with a propagation range of 3.45 km under clear air and 1.316, 1.045, and 0.7 km under rain conditions (light, medium, and heavy rain) with a received power of −12.6 dBm. As for haze conditions, the range and received power are 2.391 km with −13 dBm for low haze, 1.591 km with −12.7 dBm for medium haze, and 1.025 km with −12.6 dBm for heavy haze. The range is reduced and becomes 1.085, 0.784, and 0.645 km under fog conditions (light, medium, and heavy fog) with −12.6 dBm received power. Furthermore, the system achieved a range of 0.681, 0.232, and 0.102 km under dust conditions (light, medium, and heavy dust) with a received power of −16 dBm.

Keywords: free space optics (FSO), orthogonal frequency division multiplexing, quadrature amplitude modulation, spectral amplitude coding optical code division multiple access, enhanced double-weight code (EDW), bit error rate

1 INTRODUCTION

Orthogonal multicarrier modulation (OMCM), also known as orthogonal frequency division multiplexing (OFDM), is a data transmission technology that works well in fading and multipath networks [1]. It is also a digital multi-carrier modulation technology that can be utilized in high-data rate applications on many telecommunication protocols, including wireless communications and multimedia [2]. OFDM is based on the concept of the Inverse Fast Fourier Transform (IFFT), which requires the transmission of parallel data streams over mutually orthogonal sub-carriers with overlapping frequency bands. High spectral efficiency, inexpensive implementation, huge capacity, and resistance against both multipath and frequency selective fading and inter symbol interference (ISI) are the key advantages of OFDM technology [3].

An exponential increase in the demand for high-speed data services and an increasing number of mobile phone users make it vital to look for alternatives to the existing radio frequency (RF) infrastructure [4]. The free space optics (FSO) communication system is one of the optical communications systems that does not require any license for transmitting data but requires a line-of-sight (LOS) connection between communication endpoints. It has feasible deployment due to less power use, high security, and excessive information data rates and can be implemented in remote geographical locations [5, 6]. Due to these reasons, the FSO transmission has found its application in terrestrial transmission, inter-satellite links, and in photonic radars [7–16]. However, external weather conditions that change dynamically such as rain, haze, and fog weaken the optical signal during transmission owing to signal power absorption and scattering, decreasing the quality of the received signal [17–19].

Optical code division multiple access (OCDMA) is the most effective spread spectrum technique because of its appealing properties such as flexibility and security. Also, it can manage numerous users, offer asynchronous transmission, and simplify networks [20]. OCDMA is most commonly used in conjunction with spectral amplitude coding (SAC). Each user is assigned with unique code in SAC-OCDMA. Many codes are used in SAC-OCDMA systems, some of them have zero cross correlations which are difficult to implement such as zero cross correlation (ZCC) [21], multi diagonal [22], and random diagonal (RD) [23], whereas others have unity cross correlation such as enhanced double weight code (EDW) [24]. Unfortunately, the presence of multiple access interference (MAI) in SAC-OCDMA degrades system performance significantly, which may be alleviated by employing an appropriate detection technology (i.e., single photodiode detection technique (SPD)) [24].

The evolution of data-hungry applications like the internet of things (IoT) for smart cities that contain residential areas, agriculture farms, hospitals, different transportation means, and industrial units as displayed in **Figure 1** has challenged

FIGURE 1 | FSO-enabled smart city network [25].

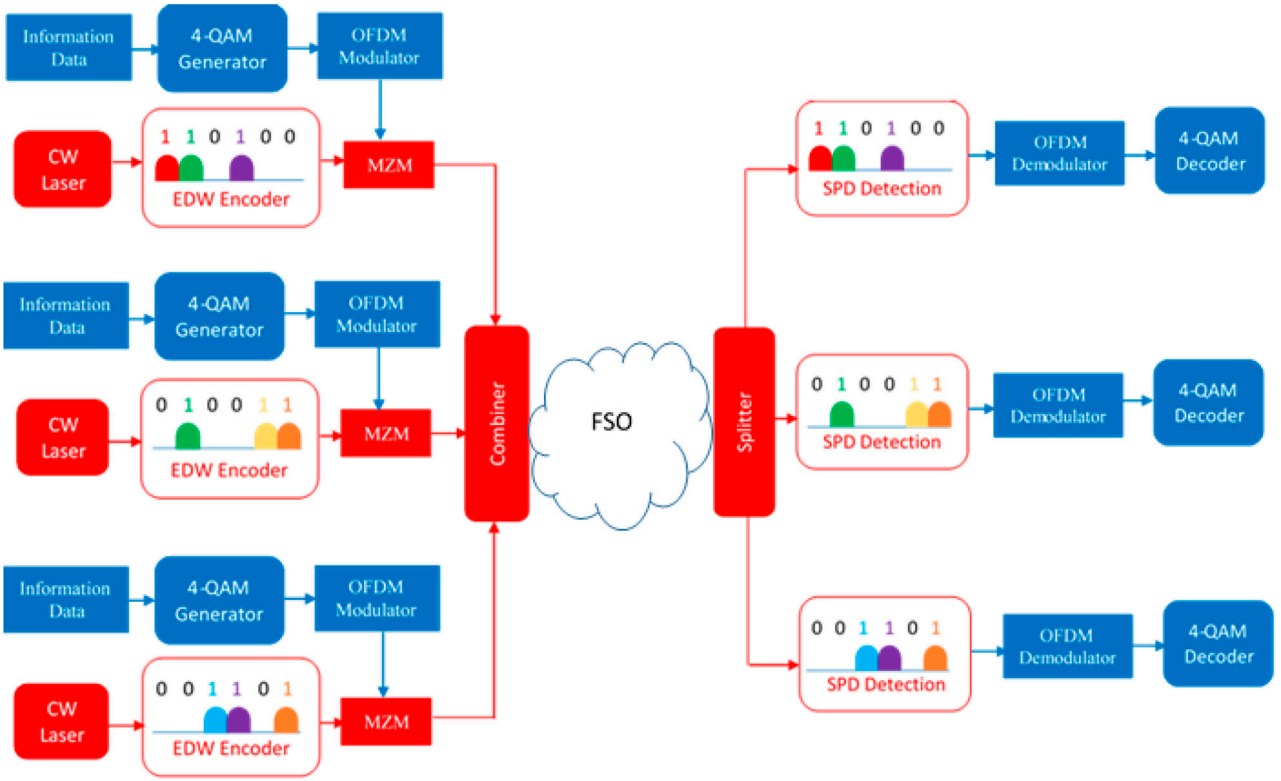

FIGURE 2 | Schematic diagram of the OFDM/SAC-OCDMA-based FSO link.

the researchers to develop new high-speed communication systems.

This article focuses on designing a novel FSO system that can be applied for implementing 5G networks. As there are places that are located in different areas having different geographical locations such as near deserts or seas or mountain, so their climate conditions will be different. For this reason, the effect of different climate conditions, i.e., clear, fog, haze, rain, and dust storm are also studied. The rest of the article is structured as follows. Literature review and research motivation are devoted in **Section 2**. The proposed system designed for evaluating the FSO link performance under various weather conditions is described in **Section 3**. **Section 4** explains the performance analysis for the proposed FSO system. The simulation results and discussion are reported in **Section 5**, followed by concluding remarks in **Section 6**.

2 LITERATURE REVIEW AND RESEARCH MOTIVATION

This section reports the previously suggested FSO systems with their conducted results and the motivation of this research.

2.1 Literature Review

In [26], the authors proposed spectrum slicing and wavelength division multiplexing (SS-WDM) in the FSO system. The obtained results reported successful transmission of 16 channels with an overall capacity of 24.96 Gbps. In [27], the authors proposed WDM in FSO communication and evaluate the performance for desert areas only and used laser power of 40 dBm, which is harmful [28]. The results showed small data transmission rates of 0.3 Gbps to 0.7 Gbps. In [22, 24], the performance of SAC-OCDMA in FSO communication is studied but with different codes, i.e., multi diagonal, ZCC, and EDW codes. The obtained results reveal low data rates as the authors used three channels, each carrying 622 Mbps, so the overall capacity is 1.866 Gbps, which is insignificant to face the excessive increase in data traffic in this decade. In addition, the system performance is limited due to the use of broadband sources and cannot propagate longer distances with higher data rates. In [29], the performance of hybrid OFDM-MDM in the FSO link using the 4-QAM scheme is evaluated. The results showed a transmission capacity of 40 Gbps, but under dust storm conditions only. In [3], the authors proposed an OFDM system with a 4-QAM signal in the FSO communication system. The obtained results revealed successful transmission of 40 Gbps, but under two weather conditions, i.e., clear air (CA) and fog conditions.

2.2 Research Motivation

The motivation of this research is to propose a hybrid OFDM/SAC-OCDMA-FSO communication system that can be used in the implementation of 5G services and smart cities. As

TABLE 1 | Rain level with attenuation [32].

Rain level	Attenuation (dB/km)
LR	6.27
MR	9.64
HR	19.28

TABLE 2 | Haze level with attenuation [34].

Haze level	Attenuation (dB/km)
LH	1.537
MH	4.285
HH	10.115

TABLE 3 | Fog level with attenuation [34].

Fog level	Attenuation (dB/km)
LF	9
MF	16
HF	22

there are areas that have different geographical locations, so, the effect of different climate conditions will be adverse. For this purpose, we study the effect of the different weather conditions in addition to considering the different FSO link parameters that can be implemented practically with less complexity.

3 PROPOSED OFDM/SAC-OCDMA-BASED FSO COMMUNICATION USING EDW CODE

The proposed model of a high-speed FSO communication system with design parameters is elaborated in this section. **Figure 2** depicts a schematic diagram of the OFDM/SAC-OCDMA-based FSO link. The proposed system consists of three main subsections:

3.1 Transmitter

In the transmitter, there is an electrical part and an optical part. As for the electrical part, a pseudo random bit generator (PRBG) is used for generating information data, that is further directed to four level quadrature amplitude modulation (4-QAM) block. A 4-QAM generator is used to create a 15 Gbps information signal with 2 bits per symbol, which is then modulated using an OFDM modulator with 512 subcarriers, 0 prefix points, and 1024 FFT points, which is then modulated with a QM modulator. In the optical part, a continuous wave (CW) laser is used to obtain the optical signals for the EDW code encoder (as an example, 110,100 for user 1). EDW code is characterized by three main parameters: unity cross correlation, λ_{cc}, any odd number >1, code weight, P, and code length, L. The codes assigned to the three users are taken from the basic matrix, M, 3×6 with $p = 3$. This is expressed as [30]

$$M = \begin{vmatrix} 0 & 0 & 1 & 1 & 0 & 1 \\ 0 & 1 & 0 & 0 & 1 & 1 \\ 1 & 1 & 0 & 1 & 0 & 0 \end{vmatrix}. \tag{1}$$

The relation between L and the number of users, C, can be expressed as [31]

$$L = 2C + \frac{4}{3}\left[sin\left(\frac{C\pi}{3}\right)\right]^2 \frac{8}{3}\left[sin\left(\frac{(C+1)\pi}{3}\right)\right]^2 + \frac{4}{3}\left[sin\left(\frac{(C+2)\pi}{3}\right)\right]^2. \tag{2}$$

The electrical signal is modulated onto the optical signal through an optical modulator (Mach-Zehnder modulator (MZM)). Then the data of the three users are combined and transmitted through the FSO channel.

3.2 FSO Channel

The FSO channel is impacted by various weather conditions such as clear, rain, haze, fog, and dust storm that cause atmospheric attenuation. As a result, these weather conditions degrade system performance during transmission.

3.2.1 Rain Conditions

Rain affects the data during transmission in the FSO channel and according to the level of rain that depends on the rainfall rate, is classified as low rain (LR), medium rain (MR), and heavy rain (HR). The different intensities of rain having different values for the rain attenuation, β_r, in dB/km are given in **Table 1** [32]. β_r can be expressed as [17]

$$\beta_r = \gamma R^t, \tag{3}$$

where R is the rain rate in mm/hr and t and γ is coefficients depending on both ambient temperature and frequency having values of 0.67 and 1.076, respectively at maximum rain intensity (100 mm/h) yielding an attenuation of ~18.3 dB/km [33].

3.2.2 Haze and Fog Conditions

Haze and fog affect the FSO link causing degradation in the received signal. Haze attenuation increases as the amount of dust or smoke particles increase in the air and can be divided into three levels, i.e., low haze (LH) which has low attenuation, medium haze (MH) which has moderate attenuation and heavy haze (HH) that have high attenuation.

The attenuation of fog increases as the number of microscopic water droplets suspended in the atmosphere increases and this makes fog heavier. So, different fog levels such as low fog (LF), medium fog (MF), and heavy fog (HF) have different attenuations.

Both haze and fog attenuation in dB/km, $\beta_{f,h}$, can be expressed as [28]

$$\beta_{f,h} = \frac{3.912}{K}\left(\frac{\lambda}{550nm}\right)^{-s}, \tag{4}$$

TABLE 4 | Dust level with visibility range [35].

Dust level	Visibility (km)
DH	≤ 10
LD	1–10
MD	0.2–1
HD	<0.2

TABLE 5 | Dust level with attenuation [29].

Fog level	Attenuation (dB/km)
LD	25.11
MD	107.66
HD	297.38

where K (km) is the range of visibility and λ (nm) is the operating wavelength. While, s denotes the size distribution of the scattering particles that can be calculated according to Kim's model as [29]

$$s = \begin{cases} 1.6 & K > 50 \\ 1.3 & 6 < K < 50 \\ 0.16\,K + 0.34 & 1 < K < 6 \\ K - 0.5 & 0.5 < K < 1 \\ 0 & K < 0.5 \end{cases}. \quad (5)$$

Tables 2, **3** show haze levels with their attenuations and fog levels with their attenuations, respectively [34].

3.2.3 Dust Conditions

Dust storm also affects the FSO link performance. According to the visibility range, World Meteorological Organization (WMO) has divided dust storms into four cases: dust haze (DH), light dust (LD), medium dust (MD), and heavy dust (HD) [35]. **Table 4** shows the visibility corresponding to these cases.

The Dust attenuation, β_D, in dB/km can be expressed as [29]

$$\beta_D = \frac{10 log T_s}{4.343\,N}, \quad (6)$$

where T_s indicates the transmittance of an optical signal at 550 nm.

Table 5 shows the different dust storm levels and their attenuation [29].

The received signal power in the FSO link is expressed as [27]

$$F_{RX} = F_{TX}\left(\frac{D_{RX}}{D_{TX} + \theta N}\right)^2 10^{\frac{-\beta N}{10}}, \quad (7)$$

where F_{TX} and F_{RX} are transmitted and received power, respectively. D_{TX} is transmitter diameter while D_{RX} is the receiver diameter. N, θ, and β, respectively, denote the FSO transmission range, the laser beam divergence angle, and the atmospheric attenuation that varies according to weather conditions.

3.3 Receiver

The receiver consists of two parts, i.e., optical and electrical. The optical part has a decoder, where detection takes place to decode the required user without MAI. Here single photodiode detection (SPD) is used. The mathematical description of MAI of SPD detection is as follows:

Suppose we consider these two code sequences code M: 001101 and code N: 010011 from the EDW code matrix given in **Eq. 1**, that have interference in the sixth bit and we want to receive code M without interference, so this interference will be canceled using SPD detection as

$C_m(i) = i^{th}$ element of code M

$C_n(i) = i^{th}$ element of code N.

The cross correlation between code M and code N will be: $\lambda_{cc}(MN) = \sum_{i=1}^{L} C_m(i)C_n(i) = \sum_{i=1}^{L}(001101)(010011) = \sum_{i=1}^{L} 000001 = 1$.

The subtractive decoder is used and contains only the interference bit between two codes as.

S-Decoder = (MN)M= (000010)001101 = 000001.

The cross correlation between the decoder that has the required spectral of the required user that is code M in this example and the S-Decoder will be: $\lambda_{cc}(Ms - Decoder) = \sum_{i=1}^{L} C_m(i)S - Decoder\ (i) = \sum_{i=1}^{L}(001101)(000001) = \sum_{i=1}^{L} 000001 = 1$Finally, the interference will be canceled as λ_{cc} (AB)−λ_{cc} (AS-Decoder) = 1—1 = 0.

After that, the optical signal passes without interference to the photodetector (PD) for optical/electrical conversion. To recover the information signal, the output electrical signal is demodulated using a QAM demodulator, followed by an OFDM demodulator, and a QAM decoder.

TABLE 6 | Simulation parameters [24, 40–45].

Parameter		Value
CW laser source	Transmitted power	15 dBm
	Linewidth	10 MHz
Information	Bit rate per user	15 Gbps
	Number of subcarriers	512
	Number of FFT points	1,024
	Sequence length	32,768
	Samples per bit	4
	Symbol rate	7.5 Gbps
	Electrical bandwidth	0.75 × Bit rate Hz
FSO channel	Transmitter aperture diameter	10 cm
	Beam divergence angle	2 mrad
	CA attenuation	0.2 dB/km
	Receiver aperture diameter	20 cm
Photodetector	PD responsivity	1 A/W
	Thermal noise power density	10^{-22} W/Hz
Noise	Boltzmann constant	1.38×10^{-23} J/K
	Receiver noise temperature	300 K
	Receiver load resistance	1,030 Ω

4 PERFORMANCE ANALYSIS

The signal from the desired user reaching PD after modulating with OFDM can be expressed as [1]

$$P_u = \frac{F_{RX} B_{op} P}{L} \sum_{n=1}^{z} C_n e^{j2\pi f_n t}, \quad (8)$$

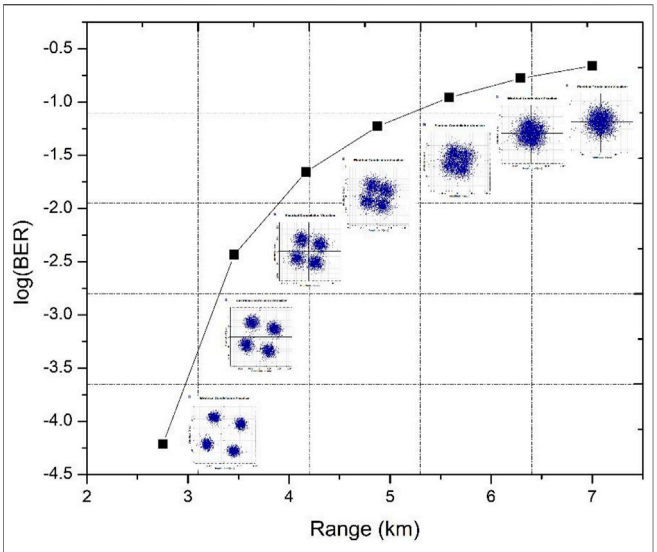

FIGURE 3 | log(BER) vs. range under CA for OFDM/SAC-OCDMA-FSO.

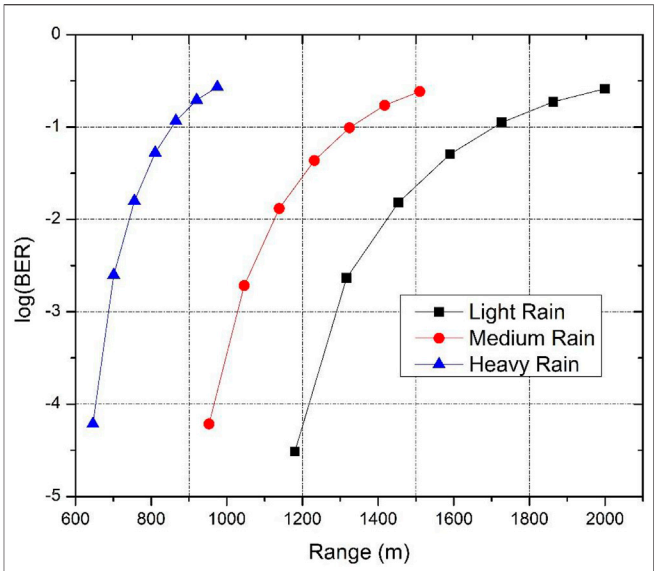

FIGURE 4 | log(BER) vs. range under different rain intensities for OFDM/SAC-OCDMA-FSO.

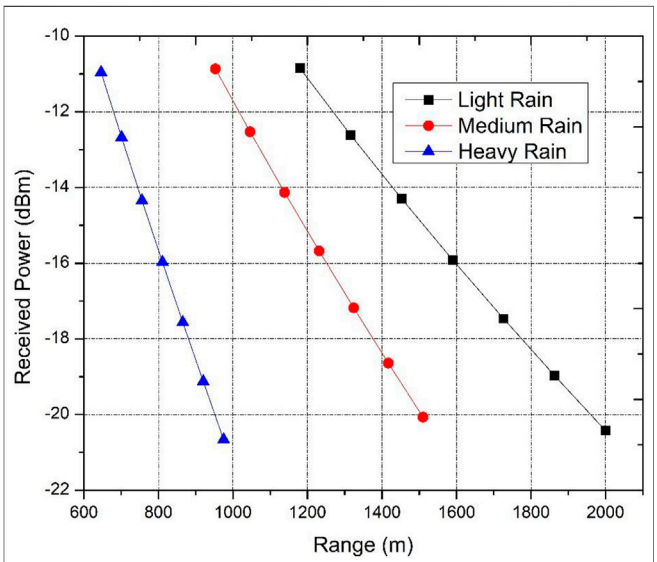

FIGURE 5 | Received power vs. range under different rain intensities for OFDM/SAC-OCDMA-FSO.

where $B_{op}n$ and C are the optical bandwidth, the number of subcarriers having a range from 1 to z, i.e., the total number of subcarriers and complex data at z subcarriers, respectively. The OFDM signal is produced by using MATLAB. For achieving the orthogonality between any two subcarriers, the following condition must be satisfied [36]:

$$f_y = \frac{y-1}{512}, \tag{9}$$

where f_y is the frequency of y subcarrier.

As the adverse climate affects the signal during transmission causing degradation, so, the signal-to-noise ratio (SNR) is reduced and the BER is increased. SNR is the ratio of mean signal power, $(P_u)^2$, to different noise source's power and is expressed as [24, 37, 38]

$$SNR = \frac{(P_u)^2}{\frac{(F_{RX})^2 B_e B_{op} P}{L} + \frac{2eB_e \Re F_{RX} B_{0p} P}{L} + \frac{4K_B T_n B_e}{R_L} + (\beta N)}, \tag{10}$$

where B_e, $\Re$, k_B, T_n, and R_L, respectively, represent the electrical bandwidth, the responsivity of the photodiode, the Boltzmann constant, the receiver noise absolute temperature, and the receiver load resistance.

Based on Gaussian approximation, the BER can be expressed in terms of SNR as [39]

$$BER = 0.5\, erfc\left(\frac{\sqrt{SNR}}{2}\right). \tag{11}$$

The recommended OFDM/SAC-OCDMA-FSO system is evaluated and simulated using Optisystem software version 18 with parameters given in **Table 6**.

5 SIMULATION RESULTS

Figure 3 shows the log (BER) for the proposed OFDM/SAC-OCDMA-FSO versus propagation range under CA weather. Also, the constellation diagram of the signal at different ranges is given in **Figure 3**. It is noted that as the link range increases, the constellation plot of the received signal becomes more distorted. The proposed system can propagate up to 3.45 km with log (BER) = −2.43, while at the 7 km range, the signal is received with a high value of log (BER).

Transmitting the data in FSO is affected by rain, so, we discuss the effect of different rain intensities on the system performance in **Figure 4**. It has been observed that as the rain intensity increases from light to heavy, the rain attenuation increases,

TABLE 7 | Maximum propagation ranges and received power under different rain conditions with log (BER) < −2.5

Rain conditions	LR	MR	HR
Range (km)	1.31	1.045	0.7
Received power (dBm)	−12.6	−12.6	−12.6

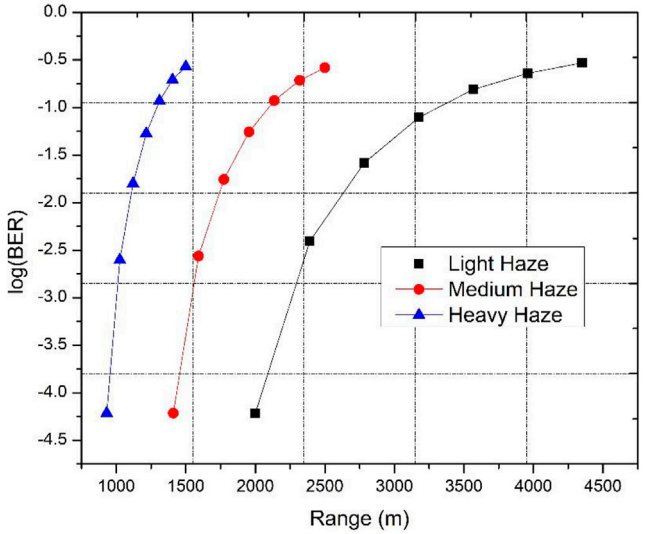

FIGURE 6 | log(BER) vs. range under various haze levels for OFDM/SAC-OCDMA-FSO.

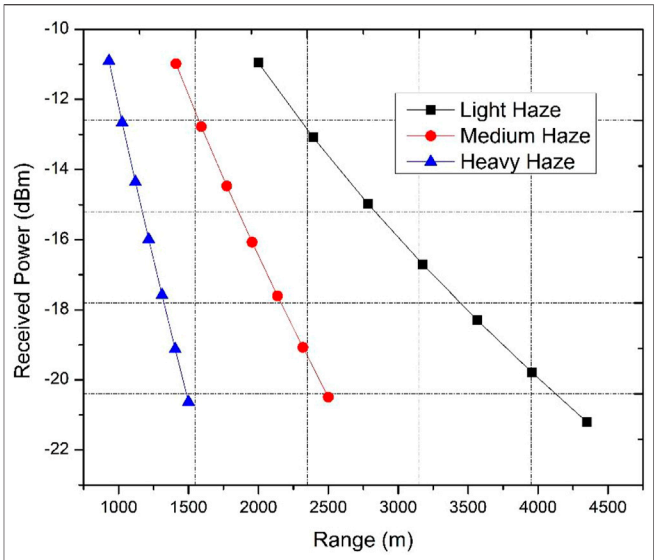

FIGURE 7 | Received power vs. range under different haze levels for OFDM/SAC-OCDMA-FSO.

TABLE 8 | Maximum propagation ranges and received power under different haze conditions with log(BER) < −2.5.

Haze conditions	LH	MH	HH
Range (km)	2.7	1.6	1.12
Received power (dBm)	−13	−12.7	−12.6

resulting in a decrease in the propagation range. When compared to MR and HR, LR has the longest propagation range as it has the lowest attenuation of 6.27 dB/km according to **Table 1**. A log (BER) ~ −2.6, LR can propagate up to 1.316 km, which is 0.271 km longer than MR and 0.616 km longer than HR at the same BER value.

Figure 5 illustrates the variation of received power for different FSO propagation ranges. As observed, the received power is maximum at the lower range while the minimum at a higher range. Also, as attenuation increases due to the increasing level of rainfall, the received power decreases. At a received power of −14 dBm, the range that the system can achieve is 1.453 km under LR, which is decreased to 1.138 and 0.755 km, under LR and MR, respectively.

Table 7 summarizes the maximum propagation ranges with corresponding received power for the proposed system under different rain conditions with log (BER) < −2.5.

The performance of the OFDM/SAC-OCDMA-FSO system is evaluated under various haze levels. **Figure 6** depicts the relationship between log (BER) values and propagation range under various haze conditions. As observed, when the amount of dust or smoke particles increases in the air, the haze level rises from light to heavy, the propagation range becomes shorter and the BER increases. The maximum range that our proposed system can propagate with log(BER) < −2.5 is 2.391 km under LH, 1.591 km under MH, and 1.025 km under HH.

Figure 7 demonstrates the received power under different haze conditions and a different range for our proposed model. As the haze attenuation is less than rain attenuation, so, the received power is higher than that achieved for rain conditions. At the same received power −14 dBm, the ranges that the FSO system can propagate are 2.7, 1.6, and 1.12 km, under LH, MH, and HH, respectively, which are greater than the range achieved under rain conditions.

Table 8 summarizes the maximum propagation ranges with corresponding received power for the proposed system under different haze conditions with log(BER) < −2.5.

Figure 8 shows log (BER) versus FSO propagation range for our model under different fog conditions. The attenuation of fog increases as the number of microscopic water droplets suspended in the atmosphere increases and this results in fog becoming heavier. Also, the attenuation causes degradation in the received signal as it increases the BER values as observed in **Figure 8**. The range that can be achieved at log (BER) values of −4.2 and −0.5, respectively, are 0.993 and 1.5 km under LF, 0.721, and 1.1 km under MF, and 0.6 and 0.87 km under HF, respectively.

Figure 9 shows the received power versus the FSO link for our proposed system under different fog conditions.

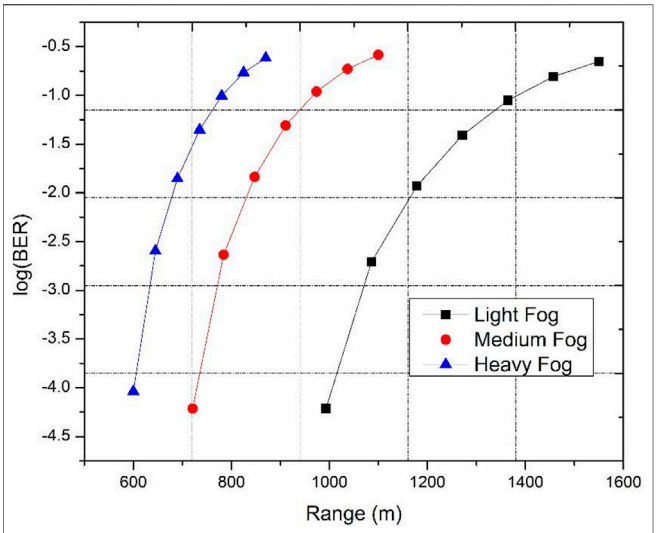

FIGURE 8 | log(BER) vs. range under different fog conditions for OFDM/SAC-OCDMA-FSO.

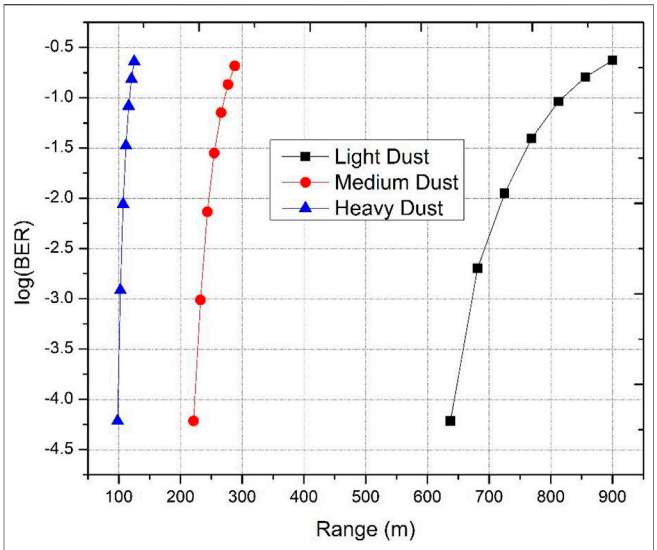

FIGURE 10 | log(BER) vs. range under dust storm conditions for OFDM/SAC-OCDMA-FSO.

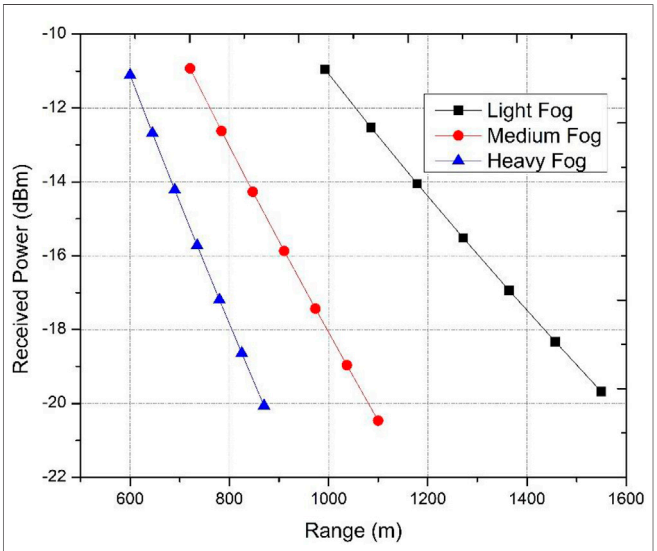

FIGURE 9 | Received power vs. range under different fog levels for OFDM/SAC-OCDMA-FSO.

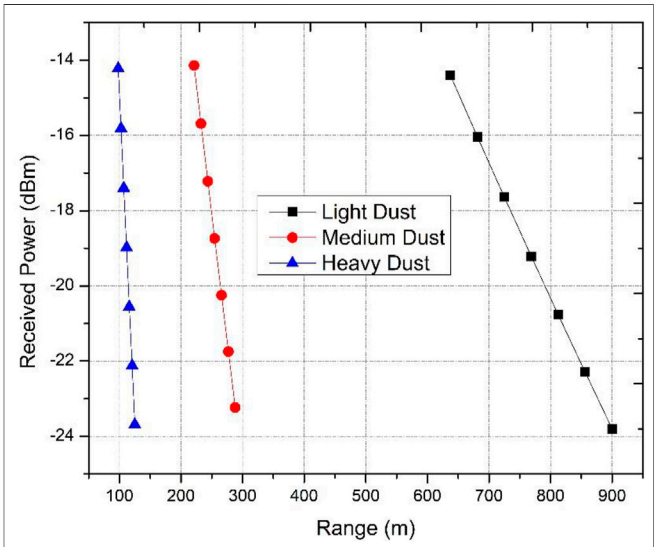

FIGURE 11 | Received power vs. range under dust storm conditions for OFDM/SAC-OCDMA-FSO.

TABLE 9 | Maximum propagation ranges and received power under different fog conditions with log (BER) < −2.5.

Fog conditions	LF	MF	HF
Range (km)	1.085	0.784	0.645
Received power (dBm)	−12.5	−12.6	−12.6

Consequently, as the HF has the highest attenuation so it achieves the shortest FSO range with optimum received power while the LF reveals the longest FSO range.

TABLE 10 | Maximum propagation ranges and received power under different dust storm conditions with log (BER) < −2.5

Dust conditions	LD	MD	HD
Range (km)	0.681	0.232	0.102
Received power (dBm)	−16	−15.6	−15.8

Table 9 summarizes the maximum propagation ranges with corresponding received power for the proposed system under different fog conditions with log (BER) < -2.5.

TABLE 11 | Comparison between past published works and our work.

References	Technique	Capacity	Weather conditions	Range (km)
Reference [41]	MDM-FSO with NRZ modulation	2 spatial modes × 5 Gbps	CA	27
			LF	2.7
			MF	1.7
			HF	1.3
Reference [46]	WDM-FSO with BSK modulation	4 λ × 2.5 Gbps	CA	231
			LR	21.5
			MR	17.4
			HR	12.7
			LF	3.7
			HF	2.3
Reference [34]	SS-WDM-based FSO with NRZ encoding	16 × 1.56 Gbps	CA	140
			LH	66
			HH	19
			LR	8.3
			MR	5.7
			HR	3.14
			LF	3.8
			HF	2.5
Present work	OFDM-SAC-OCDMA-based FSO	3 × 15 Gbps	CA	3.45
			LR	1.316
			MR	1.045
			HR	0.7
			LH	2.391
			MH	1.591
			HH	1.025
			LF	1.085
			MF	0.784
			HF	0.645

Figures 10, **11** show the log (BER) values for different FSO link range under the effect of a dust storm and the variation of received power for different propagation ranges in presence of a dust storm, respectively. It is evident from **Figure 10** that as the dust storm becomes adverse, that cause higher attenuation which is 297.38 dB/km according to **Table 2**, so, the FSO range is decreased. Maximum FSO link achieved under LD, MD and HD with log (BER) < -2.5 are 0.681, 0.232 and 0.102 km, respectively. Also, it is observed from **Figure 11** that the lighter the dust storm, the higher the achieved FSO link range and the higher the received power.

Table 10 summarizes the maximum propagation ranges with corresponding received power for the proposed system under different dust storm conditions with log (BER) < −2.5.

Table 11 shows a comparison between past published work and our work.

6 CONCLUSION

This work proposes a hybrid OFDM/SAC-OCDMA-based FSO communication system with EDW code. Three users are assigned to our model, each carrying 15 Gbps. The proposed FSO system performance employing 4-QAM modulation is investigated under different weather conditions, i.e., CA, rain, haze, fog, and dust storm. The obtained simulation results reveal that CA achieves the longest propagation range of 3.45 km. This range is reduced in the presence of rain, haze, fog, and dust storm. Under rain conditions, as the intensity of rain increases, the range becomes shorter and the obtained received power decreases. The maximum propagation ranges at −12.6 dBm received power under LR, MR, and HR, respectively, are 1.316, 1.045, and 0.7 km, respectively. In the case of haze conditions, the proposed model can propagate a range longer than that achieved under rain conditions but shorter than that achieved under CA. It extends up to 2.391, 1.591, and 1.025 km with received power of -13 dBm, −12.7 dBm, and −12.6 dBm for LH, MH, and HH, respectively. As fog has attenuation greater than CA, rain, and haze weather conditions, so the propagation range that the system achieved is decreased and become 1.085, 0.784, and 0.645 km for LF, MF, and HF, respectively at approximately −12.6 dBm received power. Moreover, the effect of dust storms is investigated with its different levels. As a dust storm has higher attenuation, the data transmission under a dust storm is received with lower power (−16 dBm). The proposed model has the potential to become a versatile and powerful technique. So, we recommend our work to be carried out in last mile access, outdoor wireless access networks, smart cities, and 5G technologies.

DATA AVAILABILITY STATEMENT

The original contributions presented in the study are included in the article/Supplementary Material; further inquiries can be directed to the corresponding author.

AUTHOR CONTRIBUTIONS

All authors listed have made a substantial, direct, and intellectual contribution to the work and approved it for publication.

FUNDING

This research was funded by the Project of Excellence of the Faculty of Science, University of Hradec Králové, grant number 2207/2022-2023.

REFERENCES

1. Aldhaibani AO, Rahman TA, Aljunid SA, Hindia MN, Hanafi EB. A New Model to Enhance the QoS of Spectral Amplitude Coding-Optical Code Division Multiple Access System with OFDM Technique. *Opt Quant Electron* (2016) 48(10):481–92. doi:10.1007/s11082-016-0750-4
2. Armstrong J. OFDM for Optical Communications. *J Lightwave Technol* (2009) 27(3):189–204. doi:10.1109/jlt.2008.2010061
3. Li C, Yang Q. Optical OFDM/OQAM for the Future Fiber-Optics Communications. *Proced Eng* (2016) 140:99–106. doi:10.1016/j.proeng.2015.09.238
4. Dat PT, Kanno A, Yamamoto N, Kawanishi T. Seamless Convergence of Fiber and Wireless Systems for 5G and beyond Networks. *J Light Technol* (2018) 37(2):592–605.
5. Shanmuga sundar D, Sathyadevaki R, Sridarshini T, Sivanantha Raja A. Photonic crystal Based Routers for Photonic Integrated on Chip Networks: a Brief Analysis. *Opt Quant Electron* (2018) 50:383. doi:10.1007/s11082-018-1655-1
6. Tang X, Ghassemlooy Z, Rajbhandari S, Popoola WO, Lee CG. Coherent Heterodyne Multilevel Polarization Shift Keying with Spatial Diversity in a Free-Space Optical Turbulence Channel. *J Lightwave Technol* (2012) 30(16):2689–95. doi:10.1109/jlt.2012.2204859
7. Chaudhary S, Kapoor R, Sharma A. Empirical Evaluation of 4 QAM and 4 PSK in OFDM-Based Inter-satellite Communication System. *J Opt Commun* (2019) 40(2):143–7. doi:10.1515/joc-2017-0059
8. Sharma A, Chaudhary N, Chaudhary S. 6 × 20 Gbps Hybrid WDM–PI Inter-satellite System under the Influence of Transmitting Pointing Errors. *J Opt Commun* (2016) 37(4). doi:10.1515/joc-2015-0099
9. Chaudhary S, Sharma A, Neetu N. 6 X 20Gbps Long Reach WDM-PI Based High Altitude Platform Inter-satellite Communication. *System" Int J Comp Appl* (2015) 122(Issue 22):41–5. doi:10.5120/21861-5192
10. Sathyadevaki R, Sundar DS, Raja AS. Photonic crystal $$4{\times }4$$ 4 × 4 Dynamic Hitless Routers for Integrated Photonic NoCs. *Photon Netw Commun* (2018) 36:82–95. doi:10.1007/s11107-018-0758-8
11. Shanmuga Sundar D, Nidhyavijay V, Sridarshini T, Raja AS. Performance Analysis of Multichannel WDM Hybrid Optical Communication for Long Haul Communication. *Frontier Res Innovation Optoelectronics Tech Industry* (2018) 347–54. doi:10.1201/9780429447082-51
12. Sharma A, Chaudhary S, Malhotra J, Parnianifard A, Wuttisittikulkij L. Measurement of Target Range and Doppler Shift by Incorporating PDM-Enabled FMCW-Based Photonic Radar. *Optik* (2022) 262:169191. doi:10.1016/j.ijleo.2022.169191
13. Sharma A, Chaudhary S, Malhotra J, Parnianifard A, Kumar S, Wuttisittikulkij L. Impact of Bandwidth on Range Resolution of Multiple Targets Using Photonic Radar. *IEEE Access* (2022) 10:47618–27. doi:10.1109/ACCESS.2022.3171255
14. Sharma A, Malhotra J. Simulative Investigation of FMCW Based Optical Photonic Radar and its Different Configurations. *Opt Quant Electron* (2022) 54:233. doi:10.1007/s11082-022-03578-y
15. Chaudhary S, Sharma A, Singh V. Optimization of High Speed and Long Haul Inter-satellite Communication Link by Incorporating Differential Phase Shift Key and Orthogonal Frequency Division Multiplexing Scheme. *Optik* (2019) 176:185–90. doi:10.1016/j.ijleo.2018.09.037
16. Chaudhary S, Tang X, Sharma A, Lin B, Wei X, Parmar A. A Cost-Effective 100 Gbps SAC-OCDMA-PDM Based Inter-satellite Communication Link. *Opt Quan Elect* (2019) 51. doi:10.1007/s11082-019-1864-2
17. Muhammad SS, Kohldorfer P, Leitgeb E. Channel Modeling for Terrestrial Free Space Optical Links". In: Proceeding of 2005 7th International Conference Transparent Optical Networks, 1. Barcelona, Spain (2005). p. 407–10.
18. Fadhil HA, Amphawan A, Shamsuddin HAB, Hussein Abd T, Al-Khafaji HMR, Aljunid SA, et al.Optimization of Free Space Optics Parameters: An Optimum Solution for Bad Weather Conditions. *Optik* (2013) 124(19):3969–73. doi:10.1016/j.ijleo.2012.11.059
19. Kim II, McArthur B, Korevaar EJ. Comparison of Laser Beam Propagation at 785 Nm and 1550 Nm in Fog and Haze for Optical Wireless Communications". In: *Proceeding SPIE 4214, Optical Wirelees Communications III* (2001). p. 26–37.
20. Sarangal H, Thapar SS, Nisar KS, Singh M, Malhotra J. Performance Estimation of 100 GB/s Hybrid SACOCDMA-FSO-MDM System under Atmospheric Turbulences. *Opt Quant Electron* (2021) 53(10):598–611. doi:10.1007/s11082-021-03257-4
21. Anuar MS, Aljunid SA, Saad NM, Hamzah SM. New Design of Spectral Amplitude Coding in OCDMA with Zero Cross-Correlation. *Opt Commun* (2009) 282(14):2659–64. doi:10.1016/j.optcom.2009.03.079
22. Mostafa S, Mohamed AE-NA, El-Samie FEA, Rashed ANZ. Performance Evaluation of SAC-OCDMA System in Free Space Optics and Optical Fiber System Based on Different Types of Codes. *Wireless Pers Commun* (2017) 96(2):2843–61. doi:10.1007/s11277-017-4327-8
23. Fadhil HA, Aljunid SA, Ahmad RB. Performance of Random diagonal Code for OCDMA Systems Using New Spectral Direct Detection Technique. *Opt Fiber Tech* (2009) 15(3):283–9. doi:10.1016/j.yofte.2008.12.005
24. El-Mottaleb SAA, Métwalli A, Hassib M, Alfikky AA, Fayed HA, Aly MH. SAC-OCDMA-FSO Communication System under Different Weather Conditions: Performance Enhancement. *Opt Quant Electron* (2021) 53(11):616–33. doi:10.1007/s11082-021-03269-0
25. Singh H, Mittal N, Miglani R, Singh H, Gaba GS, Hedabou M. Design and Analysis of High-Speed Free Space Optical (FSO) Communication System for Supporting Fifth Generation (5G) Data Services in Diverse Geographical Locations of India. *IEEE Photon J.* (2021) 13(5):1–12. doi:10.1109/jphot.2021.3113650
26. Prabu K, Charanya S, Jain M, Guha D. BER Analysis of SS-WDM Based FSO System for Vellore Weather Conditions. *Opt Commun* (2017) 403:73–80. doi:10.1016/j.optcom.2017.07.012
27. A. Ali MA, Shaker FK, Kadhum HA. Investigation and Analysis of Data Rate for Free Space Optical Communications System under Dust Conditions. *Wireless Pers Commun* (2020) 113:2327–38. doi:10.1007/s11277-020-07328-9
28. Ghassemlooy Z, Popoola W, Rajbhandari S. *Optical Wireless Communication: System and Channel Modelling with Matlab*. 2nd ed. Boca Raton, FL, USA: CRC Press (2019).
29. Singh M, Pottoo SN, Malhotra J, Grover A, Aly MH. Millimeter-wave Hybrid OFDM-MDM Radio over Free Space Optical Transceiver for 5G Services in Desert Environment. *Alexandria Eng J* (2021) 60(5):4275–85. doi:10.1016/j.aej.2021.03.029
30. Zahid AZG, Hasoon FN, Shaari S. New Code Structure for Enhanced Double Weight (EDW) Code for Spectral Amplitude Coding OCDMA System. In: Proc. 2009 International Conference on Future Computer and Communication. Malaysia: Kuala Lumpar (2009). p. 658–61. 3-5 Apr. 2009.
31. Hasoon FN, Aljunid SA, Abdullah MK, Shaari S. Spectral Amplitude Coding Systems Using Enhanced Double Weight". *J Eng Sci Technol* (2006) 1(2):192–202.
32. Chaudhary S, Tang X, Wei X. Comparison of Laguerre-Gaussian and Donut Modes for MDM-WDM in OFDM-Ro-FSO Transmission System. *AEU - Int J Elect Commun* (2018) 93:208–14. doi:10.1016/j.aeue.2018.06.024
33. Mohammed HS, Aljunid SA, Fadhil HA, Abd TH. A Study on Rain Attenuation Impact on Hybrid SCM-SAC OCDMA-FSO System. In: Proc. 2013 IEEE Conference on Open Systems (ICOS). Kuching, Malaysia (2013). p. 195–8. 2-4 Dec. 2013. doi:10.1109/icos.2013.6735073
34. Kakati D, Arya SC. Performance of Grey-coded IQM-based Optical Modulation Formats on High-speed Long-haul Optical Communication Link. *IET Commun* (2019) 13(18):2904–12. doi:10.1049/iet-com.2019.0205

35. Esmail MA, Fathallah H, Alouini M-S. An Experimental Study of FSO Link Performance in Desert Environment. *IEEE Commun Lett* (2016) 20(9): 1888–91. doi:10.1109/lcomm.2016.2586043
36. Shieh W, Djordjevic I. *OFDM for Optical Communications"*. London: Academic Press (2009).
37. Moghaddasi M, Mamdoohi G, Muhammad Noor AS, Mahdi MA, Ahmad Anas SB. Development of SAC-OCDMA in FSO with Multi-Wavelength Laser Source. *Opt Commun* (2015) 356:282–9. doi:10.1016/j.optcom.2015.07.075
38. Moghaddasi M, Seyedzadeh S, Glesk I, Lakshminarayana G, Anas SBA. DW-ZCC Code Based on SAC-OCDMA Deploying Multi-Wavelength Laser Source for Wireless Optical Networks. *Opt Quant Electron* (2017) 49(12): 393–406. doi:10.1007/s11082-017-1217-y
39. Al-Khafaji HMR, Aljunid SA, Amphawan A, Fadhil HA, Safar AM. Reducing BER of Spectral-Amplitude Coding Optical Code-Division Multiple-Access Systems by Single Photodiode Detection Technique. *JEOS:RP* (2013) 8: 13022–6. doi:10.2971/jeos.2013.13022
40. Singh M, Malhotra J, Mani Rajan MS, Vigneswaran D, Aly MH. A Long-Haul 100 Gbps Hybrid PDM/CO-OFDM FSO Transmission System: Impact of Climate Conditions and Atmospheric Turbulence. *Alexandria Eng J* (2021) 60(1):785–94. doi:10.1016/j.aej.2020.10.008
41. Zhang C, Liang P, Nebhen J, Chaudhary S, Sharma A, Malhotra J, et al.Performance Analysis of Mode Division Multiplexing-Based Free Space Optical Systems for Healthcare Infrastructure's. *Opt Quan Elect* (2021) 53(11):635–48. doi:10.1007/s11082-021-03167-5
42. Murugan KHS, Sharma A, Malhotra J. Performance Analysis of 80 Gbps Ro-FSO System by Incorporating Hybrid WDM-MDM Scheme. *Opt Quan Elect* (2020) 52(12). doi:10.1007/s11082-020-02613-0
43. Chaudhary S, Sharma A, Tang X, Wei X, Sood P. A Cost Effective 100 Gbps FSO System under the Impact of Fog by Incorporating OCDMA-PDM Scheme. *Wireless Personal Commun* (2021) 116(3):2159–68. doi:10.1007/s11277-020-07784-3
44. Zhang C, Liang P, Nebhen J, Chaudhary S, Sharma A, Malhotra J, et al.Performance Analysis of Mode Division Multiplexing-Based Free Space Optical Systems for Healthcare Infrastructure's. *Opt Quan Elect* (2021) 53:1–14. doi:10.1007/s11082-021-03167-5
45. Chaudhary S, Wuttisittikulkij L, Nebhen J, Tang X, Saadi M, Otaibi SA, et al.Hybrid MDM-PDM Based Ro-FSO System for Broadband Services by Incorporating Donut Modes under Diverse Weather Conditions. *Front Phys* (2021) 9:506. doi:10.3389/fphy.2021.756232
46. Jeyaseelan J, Kumar S, Caroline B. Performance Analysis of Free Space Optical Communication System Employing WDM-PoISK under Turbulent Weather Conditions". *J Optoelectron Adv Mater* (2018) 20(9):506–14.

Conflict of Interest: The authors declare that the research was conducted in the absence of any commercial or financial relationships that could be construed as a potential conflict of interest.

Publisher's Note: All claims expressed in this article are solely those of the authors and do not necessarily represent those of their affiliated organizations, or those of the publisher, the editors, and the reviewers. Any product that may be evaluated in this article, or claim that may be made by its manufacturer, is not guaranteed or endorsed by the publisher.